Talanta 107 (2013) 255–262

Contents lists available at SciVerse ScienceDirect

Talanta

journal homepage: www.elsevier.com/locate/talanta

Ultra-thin porous glass membranes—An innovative material for the immobilization of active species for optical chemosensors

R. Müller [a,*], N. Anders [b], J. Titus [b], D. Enke [b]

[a] CiS Forschungsinstitut für Mikrosensorik und Photovoltaik GmbH, Konrad-Zuse-Straße 14, 99099 Erfurt, Germany
[b] Institute of Chemical Technology, Universität Leipzig, Linnéstraße 3, D-04103 Leipzig, Germany

ARTICLE INFO

Article history:
Received 1 June 2012
Received in revised form
7 December 2012
Accepted 13 December 2012
Available online 17 January 2013

Keywords:
Porous silica membranes (CPG)
Optical chemosensors
Indicator immobilization
Thymol blue
Styryl acridine
Permeability

ABSTRACT

In addition to polymers, porous glasses can be used for the immobilization of indicators, chromoionophores or enzymes. Advantages of these materials include, among others, the photochemical and thermal stability. Porous glass membranes (CPG) based on phase-separated alkali borosilicate glasses with thicknesses of 250–300 μm and dimensions of approximately 9–13 mm^2 were used in this work. The average pore diameter was found to be between 12 and 112 nm. Initially, the membrane permeability for water was determined. Furthermore, the absorption spectra for the water-soaked membranes were recorded optically. CPG membranes which are pH-sensitive were prepared based on the covalent immobilization of thymol blue and a derivative of styryl acridine. In each case, the absorption spectra of the immobilized indicators are shown. The t_{90}-times vary between 4 and 20 min and were determined for the thermodynamic equilibrium. The influence of the ionic strength on the characteristic curve is discussed and detailed results are given. After the storage time of about 900 days a pH-sensitivity for a CPG membrane styryl acridine derivative sample was still detectable.

1. Introduction

For the development of optical chemosensors, it is necessary to immobilize indicators, chromoionophores, enzymes or phase-transfer accelerators to a substrate or into a matrix [1,2]. Partially contradictory requirements are set for immobilization techniques of chromophores as optical chemosensors: On one hand, the chromophore must be accessible to ions, i.e., the immobilization matrix must have a high ion permeability. On the other hand, the leaching of the indicator to or away from the matrix is undesirable. Furthermore, the immobilization framework should have tailored optical properties, such as defined transparency or scattering properties.

Besides the application of polymers [3], porous glasses were used as a matrix for immobilizing [4,5] active components. Regarding the latter, one can distinguish between sol-gel membranes and porous glasses, produced by extraction of phase separated alkali borosilicate glasses (Porous VYCOR® Glass (PVG) or Controlled Pore Glass (CPG), see [6]). In this paper only controlled pore glass is considered.

In general, following differences between polymers as immobilization matrix and porous glasses as substrate for the immobilization are given [4]:

Organic carriers are photochemically and thermally unstable, which limits the application in sensor technology since excited states may react with the surroundings. Furthermore, polymeric networks are less rigid than glass. Reactions with internal impurities such as indicators, solvents and monomers can occur, especially at high temperatures. Polymers may swell and deform, while porous inorganic materials are more stable, have a higher surface area and chemical stability. However, the ranges of indicators which can be immobilized during the process without changes in their structure are limited.

The development of pH sensors on the basis of pH colorimetric indicators, immobilized onto porous glasses, was the subject of several studies. Baldini and Falai [7] proposed an optical-fibre pH sensor with methyl red as optical indicator. Methyl red was immobilized on CPG particles. In the first step, the surface of the CPG was modified with γ-aminopropyl-triethoxysilane. Afterwards, methyl red was covalently bound to the modified glass surface. Finally, the CPG particles were fixed on a plastic reflector. In comparison to former systems, the optical-fibre pH sensor showed several advantages. The working range of the sensor was quite broad. The authors observed a linear relationship from pH=3 up to pH=8. No leakage of the pH-sensitive dye from the CPG matrix was observed. The plastic reflector with the immobilized CPG particles could be replaced easily. Additionally, the sensor was characterized by a fast response time.

Several pH indicators, immobilized onto CPG particles with different pore diameters, were used as components of fibre-optic biosensors for the determination of different pesticides in fruits or vegetables [8,9]. The sensors are based on the inhibition of the

* Corresponding author. Tel.: +49 36 1663 1430.
E-mail address: rmueller@cismst.de (R. Müller).

0039-9140/$ - see front matter © 2013 Elsevier B.V. All rights reserved.
http://dx.doi.org/10.1016/j.talanta.2012.12.038

Table 1
Physical properties of the appropriated CPG membranes.

	Specific surface area [m^2/g]	Specific pore volume [cm^3/g]	Porosity[a] [%]	Average pore diameter [nm]	Membrane thickness [μm]
CPG I	179*	0.56*	55*	12*	300
CPG II	66*	0.47**	51**	47**	300
CPG III	27*	0.45**	50**	66**	270
CPG IV	26*	0.56**	55**	112**	250

[a] Calculated with 2.2 g/cm^3 for skeletal density of the CPG-membranes (determined by helium pycnometry).
* Determined by low temperature nitrogen adsorption.
** Determined by mercury intrusion.

immobilized enzyme acetylcholinesterase by various pesticides. The enzyme-catalyzed substrate degradation is used for the detection of the enzyme activity. In the absence of pesticides, the enzyme is more active and therefore the hydrolysis of the substrate occurs faster. The formed acetic acid decreases the pH in the solution, which is detected by the pH-sensitive indicator. In the presence of different amounts of pesticide, the enzyme activity is reduced. Under comparable conditions it results in a less decreasing pH value. The concentration of the pesticide is proportional to the changes in the pH value. In this sensor concept, the immobilized pH indicator acts as optical transducer of the enzyme's inhibition by the corresponding pesticide. Xavier et al. [8] immobilized chlorophenol red onto diazotized CPG particles with 70 nm pore diameter. The modified CPG was placed at the common end of a bifurcated fibre optic bundle, which was then integrated in a flow-through cell. The CPG/indicator component showed a broad working range between pH=4 and pH=9.5. This was sufficient to detect the pH changes through the enzyme-catalyzed reaction. In an earlier study, Andres and Narayanaswamy [9] covalently immobilized thymol blue onto aminopropyl CPG beads with 50 nm pore size through a condensation reaction with formaldehyde. The bioactive component of the sensor consisted of a mixture of CPG beads loaded with immobilized acetylcholinesterase or thymol blue. As thin layer the glass bead mixture was packed at the tip of a bifurcated fibre optic sensor head, which was again placed in a flow-through cell. The working range of the CPG/indicator component was not specified.

In this work, porous glass membranes, prepared by extraction of phase-separated alkali borosilicate glasses (CPG membranes), were tested as a matrix for the immobilization. Compared to granular particles, membranes show the following advantages:

- favorable optical and handling properties due to plane parallel shape
- best reproducibility of the indicator–membrane-complex's properties
- simple combination of multiple functional layers in a sensor
- possibility of changing individual membranes in order to regenerate the functional species or to practice a disposable concept.

The suitability of the CPG membranes as immobilization matrix for dyes will be demonstrated exemplary using the immobilization of thymol blue and a styryl acridine derivative. Porous membranes with pore diameters in the range of 12 to 112 nm were used and characterized.

2. Experimental part

2.1. Materials

2.1.1. CPG membranes

In comparison to sol–gel membranes or layers, which are preferably used as components of optical chemosensors, porous glass membranes based on phase-separated alkali borosilicate glasses show several advantages:

- narrow pore size distribution,
- controllable pore size in a broad range between 2 and 200 nm,
- good reproducibility in the textural properties (pore structure),
- high hydrolytic stability.

However, porous glass membranes are commercially available only as Porous VYCOR® Glass (PVG) with a pore size of about 4 nm. This limits the use of PVG membranes in many sensor applications (bulky functional species, accessibility for the analyte, response time). To overcome this limitation, porous glass membranes with a controlled pore size (CPG) in the range between 12 and 112 nm were used. In this work porous glass membranes (thickness d=250–300 μm) were used, for the first time, as hydrophilic carrier for the immobilization of pH-sensitive dyes whereas the membranes themselves act as mechanical support. The amount of immobilized indicator as well as the accessibility of the functional species could be optimized by variation the textural material properties. The properties of the different porous glass (CPG) membranes are summarized in Table 1.

The manufacturing process of the CPG membranes is described in [10]. Initial glass blocks with a composition of 70 wt% SiO_2, 23 wt% B_2O_3 and 7 wt% Na_2O and a lateral block size of 9 × 13 mm^2 were used for the preparation of the CPG membranes. A typical composition of this porous network was 94.5 wt% SiO_2, 5.3 wt% B_2O_3 and 0.2 wt% Na_2O. The texture properties of the CPG membranes were determined by mercury intrusion and low temperature nitrogen adsorption.

2.1.2. Used chemicals

The silane (γ-aminopropyltriethoxysilane) and dimethylformamide (DMF) were purchased from Fluka (Steinheim) in p.a.-quality. Thymol Blue, 2-(4-morpholino)ethanesulfonic acid; (MES; biological buffer solution, pH=6.1) and formaldehyde (CH_2O; 37 wt% in H_2O) in p.a.-quality were received from Sigma (Neu-Ulm). Different buffer solutions where used to analyze the pH-sensitive behavior of the membrane/indicator complex and the influence of the ionic strength. The buffer solutions were prepared according to Coch Frugoni [11]. The styryl acridine derivative is described in Section 2.2.4. All chemicals used but not mentioned in this chapter were of analytical grade.

2.2. Characterization and modification of CPG membranes

2.2.1. Water permeability

The permeability of distilled water at 25 °C was calculated after Darcy (Eq. (1)) for some selected CPG membranes. That parameter is significant for flow through membrane sensors [12]. The membrane

was positioned onto a homemade setting where the margins were sealed with silicon (Elastosil® E10, Wacker silicone). A hydrostatic pressure was induced above the membrane, while the adjusted flow rate below the membrane was detected gravimetrically. The perfused area was always between 80 and 90 mm^2.

$$V/t = k \times A/\eta \times p/d \quad (1)$$

V/t	Flow rate [$L\ s^{-1}$]
k	Permeability [mm^2]
A	perfused membrane area [m^2]
η	dynamic viscosity of water (25 °C) [Pa s]
p	pressure difference [Pa]
d	membrane thickness [m]

2.2.2. Optical properties

To analyze the optical properties a CPG membrane was fixed perpendicular to the course of beam onto a special Teflon holder in a disposable cuvette. The measurements were performed in distilled water. UV/vis-measurements were conducted using a Lambda II-Spectrometer (Fa. Perkin Elmer, Überlingen) to gain the extinction E for a wavelength spectrum. Measurements were carried out at room temperature (21 ± 1 °C). Each prepared cuvette was filled with distilled water 24 h before measuring.

2.2.3. Immobilization of thymol blue

The amino-silanized CPG membranes were prepared according to the procedure of Foltynowicz et al. [13]. First a 10 wt% solution of γ-aminopropyltriethoxysilane (γ-APTS) in distilled water was produced. Each CPG membrane was placed into a 20 mL beaker and covered with 1.5 mL of the γ-APTS solution. The reaction took place at 80 °C for 2 h. This was followed by repeated washing steps with distilled water and a final washing with acetone, each in an ultrasonic bath for 10 min. Afterwards the membranes were dried for 14 h at 110 °C. Thymol blue was immobilized on CPG I and CPG II samples (see Table 1) as follows [9]:

The modified CPG membranes were kept in a 25 mL weighing bottle. A volume of 20 mL of a 0.1 M MES-solution (biological buffer solution, pH=6.1) were mixed with 20 mg of formaldehyde (CH_2O, 37 wt% in water) which corresponds to 10 mM CH_2O in 0.1 M MES. A volume of 1 mL of this solution was added into the weighing bottle. Furthermore 1 mL of a 5 mM aqueous solution of thymol blue was added. The sealed weighing bottles were stored for 48 h at 60 °C. Subsequently the functionalized CPG membranes were washed with distilled water in the manner described above. The studies concerning the pH-sensitivity of the CPG/indicator complexes have been conducted as described in Section 2.2.2.

The prepared cuvettes with integrated pH-sensitive CPG membranes were filled with buffer solution and conditioned under exclusion of light at room temperature for at least 24 h. After this the first measurements were made. The following storage was carried out under the terms of conditioning. All measurements were performed at room temperature (21 ± 1 °C).

Unless specified otherwise, the absorbance values used to display characteristic curves $E=f$ (pH) were determined under equilibrium conditions. The equilibrium's adjustment was detected through preliminary investigations at the wavelength of maximum absorption of the respective indicator's protonated form.

2.2.4. Immobilization of a styryl acridine derivative

The nitrogen-hydroxysuccinimide (NHS) activated styryl acridine derivative 6-[2-((*E*)-acridine-9-yl-vinyl)-5-diethylamino-phenoxy]-hexanoic acid *N*-succinimidyl ester (see Fig. 1, manufacturer: Dyomics GmbH—Jena, Germany, briefly: BS121) was linked covalently to CPG II–IV.

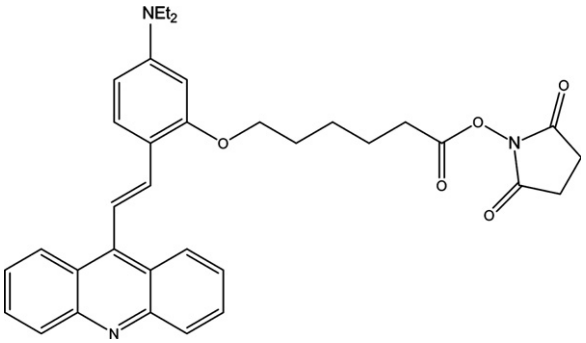

Fig. 1. NHS activated styryl acridine derivative BS121 (deprotonated form).

Table 2
Strategies to immobilize the NHS activated styryl acridine derivative.

Type of membrane	Concentration of indicator in DMF [mmol]	Reaction time [h]	Previous washing in acetone
CPG II	1.30	72	No
CPG III	0.25	20	Yes
CPG IV	0.25	20	Yes

Cocktails containing various concentrations of the indicator dissolved in anhydrous dimethylformamide (DMF) were prepared to immobilize the indicator. The aminosilanized CPG membranes were covered with 0.8 mL of the respective cocktails and stored at room temperature for a defined period of time under light exclusion in sealed weighing bottles (see Table 2). The preparation of cocktails and the coating of the membranes were done under N_2 atmosphere. Some CPG membranes were washed with acetone and dried at 40 °C to reduce the adsorption of water due to air humidity. Finally the membranes were placed into the weighing bottles without removing them out of the oven.

The resulting CPG/indicator complexes were washed for 5 min with pure ethanol and distilled water in an ultrasonic bath. The complexes' conditioning and storage occurred at pH=8.5. The pH-sensitivity of the complexes was performed as described in Section 2.2.3.

3. Results and discussion

3.1. Permeability

The permeability for water was determined gravimetrically for CPG II and IV. According to Eq. (1) the permeability k is indicated in units of mm^2 (see Tables 3 and 4).

Eq. (1) is valid only for laminar flow and if interactions between the fluid and the pore walls can be neglected. It is assumed that the second point is not fulfilled, and therefore k could not be determined as a constant for CPG II and CPG IV.

In addition, other phenomena such as thermal creep, electrokinetic, viscous heating, anomalous diffusion, and even quantum and chemical effects may be responsible for the variations of k [14].

The gravimetrically determined flow rates and permeabilities were checked using the law of Hagen–Poiseuille [Eq. (2)].

$$(V/t)_{th} = (\pi \times r^4/8 \times \eta \times d) \times p \quad (2)$$

r	pore radius [m]
$(V/t)_{th}$	theoretically calculated flow rate for one pore

η dynamic viscosity of water (25 °C) [Pa s]
p pressure difference [Pa]
d length of the straight cylindrical pore, corresponds to the membrane thickness [m]

The results are shown in Table 5. First, a theoretical flow rate was calculated for a single straight cylindrical pore by means of the mean pore radius (see Table 1). Using the volume of a straight cylindrical pore and the porosity one can calculate the theoretical number of such pores. Multiplication with that value results in the calculated flow rate $(V/t)_{\text{all pores}}$. A theoretically calculated permeability k can be given by using Eq. (1).

Comparing the calculated values in the fifth row of Table 5 with the measured data in Tables 3 and 4 the flow rates have the same magnitude. Due to the linear linkage in Eq. (1), this also applies to the theoretical and experimental permeabilities k.

As noted above, the use of Eq. (2) in combination with the calculations in Table 5 represents one opportunity to predict the flow of aqueous solutions through the porous glass membranes.

It can be resumed that the water permeability shows the "Poiseuille flow" over all determined pore radii. Concrete limitations restrictive models in this respect were discussed above in connection with [14].

Table 3
Permeability of water for a CPG II membrane according to Eq. (1), perfused area $A=79$ mm^2, membrane thickness $d=300$ µm, $\eta_{H_2O}=1\times10^{-3}$ Pa s (25 °C).

Pressure difference $p\times10^{-3}$ [bar]	Flow rate $(V/t)_{exp}$ gravimetric calculated* [mm^3 min^{-1}]	Measured permeability* $k\times10^{-11}$ according to Eq. (1) [mm^2]
25	0.80	2.03
49	1.40	1.81
74	2.05	1.75
98	2.60	1.68
123	3.20	1.65

* Average of five measurements.

Table 4
Permeability of water for a CPG IV membrane according to Eq. (1), perfused area $A=88$ mm^2, membrane thickness $d=250$ µm, $\eta_{H_2O}=1\times10^{-3}$ Pa s (25 °C).

Pressure difference $p\times10^{-3}$ [bar]	Flow rate $(V/t)_{exp}$ gravimetric calculated* [mm^3 min^{-1}]	Measured permeability $k\times10^{-11}$ according to Eq. (1) [mm^2]
25	6.4	12.10
49	12.1	11.70
74	15.8	10.10
98	19.8	9.57
123	23.4	9.01

* Average of respectively five measurements.

3.2. Optical absorption behavior

The UV-vis spectra of the four used porous glass membranes are shown in Fig. 2.

The average dimensions of the silica/water interfaces in the pore system are below the used wavelength. Refraction, diffraction, Fresnel reflection and scattering of electromagnetic radiation caused by interfaces can be observed. These effects have a growing influence for a decreasing wavelength or an increasing average pore diameter.

The extinction of the CPG membranes is important for sensor applications. A lower extinction is to be preferred for transmission models. Regarding this, CPG membranes with <50 nm average pore diameter are better suited for optical sensor applications. But the response time is another important fact for characterizing the properties of optical chemosensors. Here membranes with larger pore sizes have an advantage. This means that these contrary properties must be optimized for a given sensor application. The great variability of the membranes textures is a benefit compared to other porous substrates used for optical chemosensors.

3.3. pH-sensitive CPG membranes

3.3.1. CPG/thymol blue complexes

Thymol blue was immobilized on modified CPG I and II to test the suitability of the resulting CPG/indicator complexes for optical pH measurements. The absorption spectra of thymol blue on the CPG membranes for different pH values are shown in Fig. 3.

This figure shows that porous glass membranes are a suitable matrix for the immobilization of the indicator. The formation of an isosbestic point shows that the two types of the indicator (protonated/deprotonated) are formed according to the respective pH value. Comparable absorption spectra were obtained after 200 days of storing the complexes in a buffer solution. This

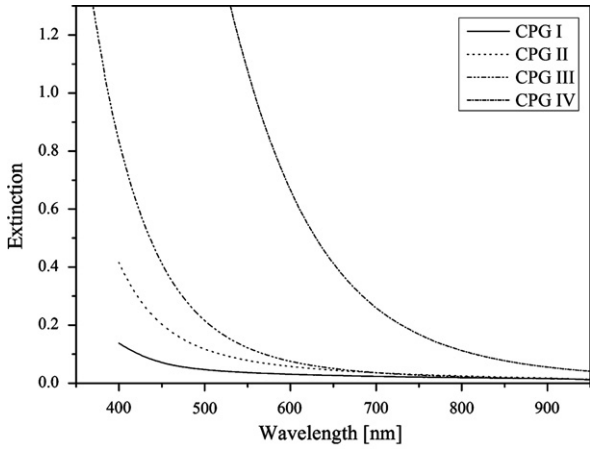

Fig. 2. UV–vis spectra of porous glass membranes in water.

Table 5
Theoretical calculation of the throughflow volume of two CPG membranes [average pore radius, membrane thickness and porosity according to Table 1, $p=0.123$ bar, $\eta_{H_2O}=1\times10^{-3}$ Pa s (25 °C)].

Type of membrane (perfused area)	Flow rate $(V/t)_{\text{one pore}}$* [mm^3 min^{-1}]	Volume of one pore [mm^3]	Theoretical number of straight cylindrical pores**	Flow rate $(V/t)_{\text{all pores}}$ [mm^3 min^{-1}]	Theoretical permability $k\times10^{-11}$ [mm^2]
CPG II (79 mm^2)	3×10^{-10}	5.2×10^{-10}	23.2×10^9	6.9	3.48
CPG IV (88 mm^2)	114.5×10^{-10}	24.6×10^{-10}	4.9×10^9	56.4	29.20

* According to Eq. (2).
** Due to the membranes porosity the determined theoretical volume of all pores is smaller than the pore volume found in closest packing's.

underlines the high long-term stability of the immobilized indicator and represents an important prerequisite for later practical applications. Due to the highest specific surface area (Table 1) the largest amount of indicator was immobilized on CPG I. The conflict between self-absorption of the CPG membrane and absorption capacity of the indicator ascends with increasing average pore diameter.

3.3.2. CPG/styryl acridine derivative complexes

As described above, the NHS activated styryl acridine derivative BS121 (Fig. 1) was covalently bound to CPG II–IV. The corresponding absorption spectra and calibration curves $E=f$ (pH) for CPG II are shown in Fig. 4.

The results presented in Fig. 4 indicate that one can reach significantly higher absorption levels with immobilized functionalized styryl acridine than with thymol blue. Causes are the lower concentration of thymol blue in the immobilization solution and the best steric conditions for the formation of covalent bonds between the functionalized styryl acridine BS121 and amino-silanized pore surface. Both forms of the indicator (protonated and deprotonated) are spectroscopically detectable after immobilization. This means that the applied immobilization procedure is optimal for the used styryl acridine derivative. Furthermore, it can be stated that pH-sensitive CPG membranes retain their functionality over several years, during storage in a slightly alkaline solution. The existence of both protonated and deprotonated form could still be detected after 30 months.

Fig. 5 shows the time course of extinction during variation of the pH values for CPG II/BS121 complexes. With regard to the dynamic response times it is assumed that the shown diffusion processes in the pore system of the CPG membranes mainly determine the response time.

A plane-parallel structure of the membrane phase can be assumed. The membrane is able to adsorb or emit particles from or into a further phase, until a concentration equilibrium between membrane phase and the adjacent phases is reached. According

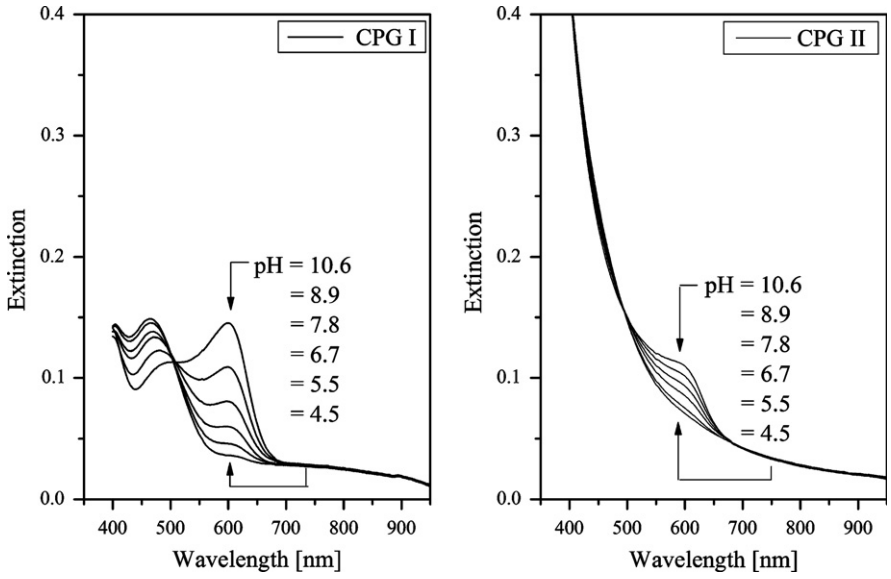

Fig. 3. Absorption spectra of thymol blue immobilized on CPG I (left) and CPG II (right) for different pH values, $I=0.1$ M, 5 days after immobilization.

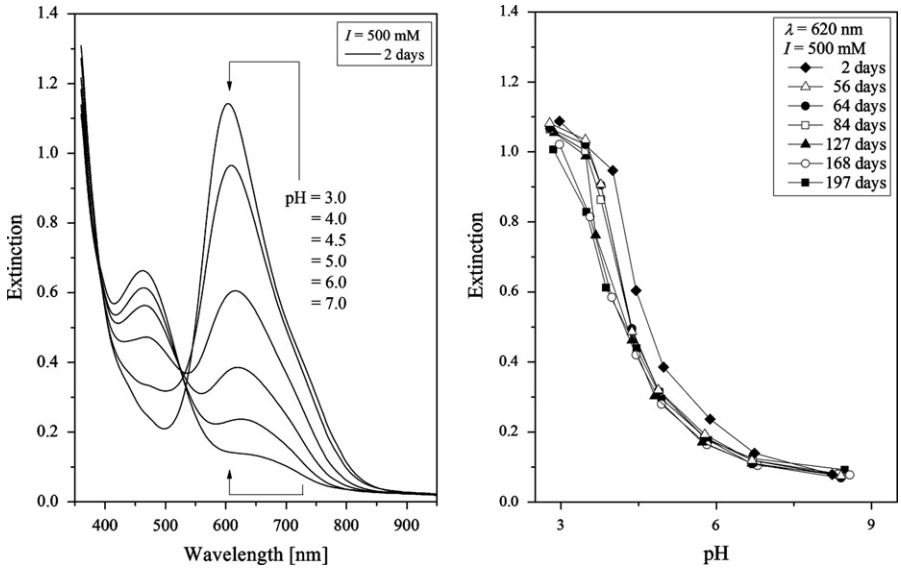

Fig. 4. Absorption spectra of styryl acridine derivative BS121 immobilized on CPG II during variation of the pH value ($I=0.5$ M) after 2 days of storage (left), calibration curves after different periods of storage at pH=8.5 (right).

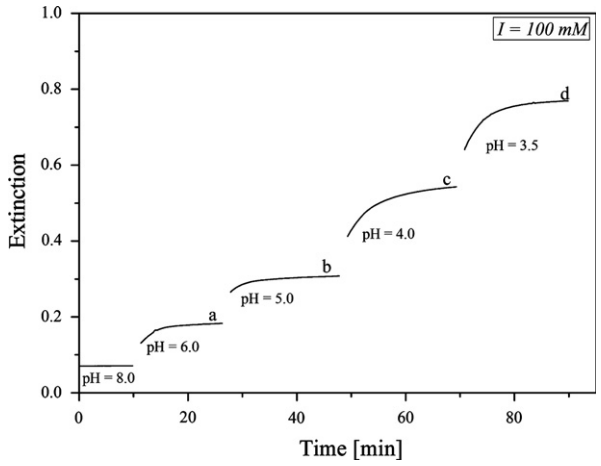

Fig. 5. Time course of extinction during variation of the pH values for BS121 immobilized on CPG II (sample 2), λ=620 nm, 30 days storage, t_{90}-times in min.: (a) 5.3; (b) 6; (c) 10.6; (d) 8.

to [15], Eq. (3) can be applied on the basis of Fick's laws. The concentration of particles in the adjacent phase is assumed to be constant. The diffusion takes place perpendicular to the planar interfaces between two phases. The diffusion across the margins of membranes is neglected.

$$D = (-\ln(0.1 \times \pi^2/8) \times d^2{}_M)/\pi^2 \times t_{90} \quad (3)$$

D diffusion coefficient of the particle in the membrane phase [$m^2\ s^{-1}$]
d_M geometric thickness of the membrane phase [m]
t_{90} period of time in which the concentration compensation achieved 90% [s]

Eq. (3) can be transferred to the kinetic processes in Fig. 5. This means that an indirect proportional relationship exists between the specified t_{90}-times and the effective diffusion coefficient for hydrated ions in the pore system D_{CPG} (d_M=300 μm). In the best case of the t_{90}-time of 5.3 min the diffusion coefficient D_{CPG} results in $0.6 \times 10^{-10}\ m^2\ s^{-1}$ while in the worst case a t_{90}-time of 22.7 min results therefore in a diffusion coefficient D_{CPG} of $0.14 \times 10^{-10}\ m^2\ s^{-1}$. The following ratios D_I/D_{CPG} can be calculated. D_I is the diffusion coefficient of hydrated ions without interferences in the used buffer solutions. According to [16] the diffusion coefficient for HCl (c=0.1 M) dissolved in water D_I is $3.1 \times 10^{-9}\ m^2\ s^{-1}$ [11]. Calculating the ratio with t_{90} (5.3 min) the ratio D_I/D_{CPG} equals 52, while for a t_{90}-time of 22.7 min the ratio arises to 221. The self-diffusion coefficient's ratio for a liquid (water, methanol) without $\overline{D}_{free}$ and with the influence of a pore system $\overline{D}_P$ was determined for CPG granules in [17]. The authors found $\overline{D}_{free}/\overline{D}_P \approx 2$ or ≈ 4 (for water molecules at 20 °C) for an average pore diameter of 45 nm or 5.8 nm.

Obviously the interactions of the pore interface (surface) with hydrated ions are larger than with uncharged species. In addition, the self-diffusion coefficient and the diffusion coefficient for specific molecules or dissolved electrolytes are not always consistent.

Finally, it can be noted that thinner CPG membranes should lead to shorter response times, since the influence of the membrane thickness d_M is quadratic in Eq. (3).

The corresponding absorption spectra and curves of $E=f$ (pH) for the CPG III/BS121 and CPG IV/BS121 complexes are shown in Figs. 6 and 7. The indicator concentration was lower for the immobilization in these two cases than in the combination of CPG II/BS121 (see Table 2).

Due to the higher background absorption of CPG III, the absorption band of the deprotonated form of BS121 is distorted and compressed (Fig. 6). However, the absorption band of the protonated form remains substantially unchanged.

As a result of the drastic increase in intrinsic absorption of CPG IV with respect to CPG II the absorption band of the deprotonated BS121 form is no longer detectable (Fig. 7). The absorption band of the protonated form is less distorted and compressed.

The wavelengths of the maximum adsorption of the protonated form of the immobilized dye show dependence on the pH value (Figs. 4 and 6). The corresponding wavelength decreases with decreasing pH value. This effect can be explained as follows. Styryl acridine derivatives show a hypsochromic behavior. The wavelength of maximum adsorption decreases with an increasing polarity of the micro-environment of the immobilized dye. The protonation of further surface species in the vicinity of the dye molecules is a possible explanation.

The influence of ionic strength [11] on the characteristic line $E=f$ (pH) (cp. Figs. 6 and 7 right) can be discussed in the following way. The used styryl acridine derivate induces an equilibrium reaction as follows:

$$HA^+ + H_2O \rightleftharpoons H_3O^+ + A^0 \quad (4)$$

The deprotonated form A^0 is an electrically neutral substance. Moreover the positive charge of the protonated form HA^+ is delocalized. If the law of mass action is applied on Eq. (4) and the dissociation constant K of the indicator is calculated, by the logarithm, one obtains Eq. (5).

$$pH = pK + \lg(c_{A0}/c_{HA+}) + \lg(f_{A0}/f_{HA+}) - \lg(a_{H_2O}) \quad (5)$$

K dissociation constant
c concentration (mol L^{-1})
f activity coefficient
a activity

If the pH sensitive CPG membrane is calibrated with a specific buffer solution series possessing a constant ionic strength, one can determine the pH value via identification of c_{A0} or c_{HA+} by using a spectrometer. The quotient f_{A0}/f_{HA^+} can be changed via variation of the ionic strength of the buffer solution at constant pH. According to the Debye–Hückel equation the activity coefficient of charged species is more influenced by the ionic strength of the surrounding than the coefficient of the uncharged species. This means that f_{HA+} decreases with increasing ionic strength and f_{A0} remains almost constant.

An apparently higher pH value is measured if the ionic strength of the medium increases. Bates [18] obtained such effects by varying the ionic strength from I=0.1 M to I=0.5 M for methyl yellow, neutral red or Nile blue. These indicators reacted in aqueous solution according to Eq. (4). Changes in the range of pH=0.05 in were observed in the transition point of the sigmoidal curves.

It was found that a pH variation of approximately 0.6 pH units was obtained from Fig. 6 (right) for the transition from the ionic strength of 100 mM to an ionic strength of 20 mM. But how can such a drastic effect of ionic strength arise? The equilibrium between protonated and deprotonated form of the indicator adjusts between the volume of the solution and the glass surface (gs). In this case Eq. (5) is to be formulated in the following form [19]:

$$pH_{gs} = pK_{gs} + \lg(c_{A0}/c_{HA+})_{gs} + \lg(f_{A0}/f_{HA+})_{gs} - \lg(a_{H_2O})_{gs} \quad (6)$$

This means that all previous statements, which are related to Eq. (5), must be transferred to Eq. (6). Thus, the activity of water in boundary layers is not negligible. Furthermore, ions can be specifically adsorbed on surfaces. In addition, the activity

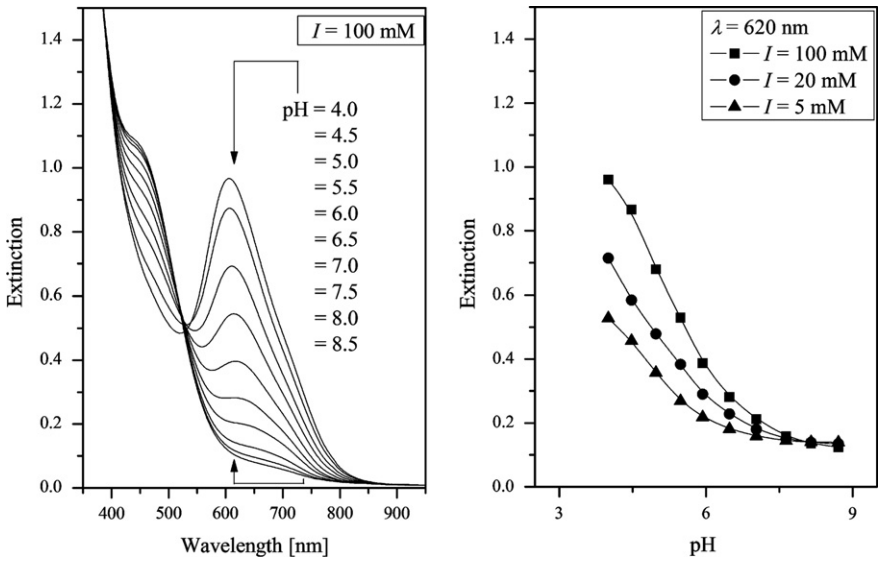

Fig. 6. Absorption spectra of styryl acridine derivative BS121 immobilized on CPG III during variation of the pH value (left), calibration curves for three different ionic strengths (right).

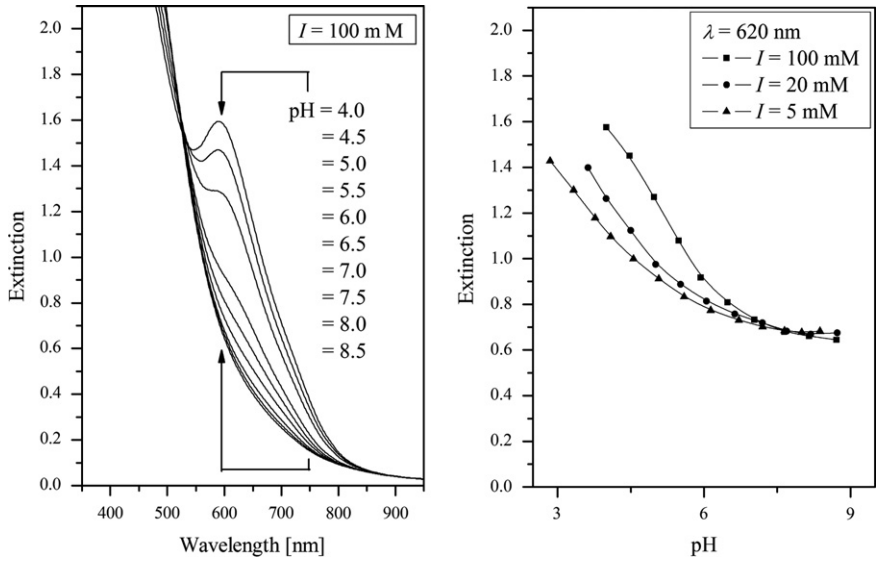

Fig. 7. Absorption spectra of styryl acridine derivative BS121 immobilized on CPG IV during variation of the pH value (left), calibration curves for three different ionic strengths (right).

coefficients of species, which are located on a surface or in an interface, differ from the values in the bulk phase (*bp*).

The following relationship exists for a_{H^+} respectively the pH value:

$$\mathrm{pH}_{gs} = \mathrm{pH}_{bp} + N \times e \times \psi / RT \times \ln 10 \quad (7)$$

N	Avogadro constant [mol^{-1}]
e	elementary charge [As]
ψ	surface potential [V]

The surface potential depends on the concentration gradient of all ionic species, which are located at the interfaces. Thus each ionic species adsorbed in the interface influences the value on pH_{gs}. Furthermore, the surface potential is codetermined from ionizable groups, which are located directly on the substrate surface. The density of ionizable groups directly depends on the chemical composition and the morphology of the surface.

For further discussion it is assumed that the activity coefficient of the uncharged deprotonated form of the styryl acridine derivative $(f_{A^0})_{gs}$ is constant related to the interface inside the pores. Furthermore it is assumed that the activity of water $(a_{H_2O})_{gs}$ (referred to the interface in the pores) is not affected by variations of the ionic strength.

With these assumptions, the change of the activity coefficient of the protonated form of styryl acridine $(f_{HA^+})_{gs}$, in relation to the interface in the pores, is responsible for the influence of the ionic strength on the characteristic shape of the pH curves.

This means $(f_{HA^+})_{gs}$ is more influenced by the ionic strength than the activity coefficient of the positively charged form f_{HA+}, for example of methyl yellow, neutral red or Nile blue in aqueous solution.

The surface charge density σ at the interface of the pores must be taken into account for a coherent explanation. The pH value and the ionic strength control the value of the surface charge density σ at the interfaces of the CPG membranes [20,21]. The

influence of these parameters was investigated for VYCOR 7930® [22,23]. At a certain pH value one observes the formation of a point of zero charge ($pH_{\sigma=0}$).

The surface chemistry is very complicated in the case of CPG membranes with an immobilized indicator. Remaining silanol groups exist alongside aminopropyl groups (from the first modification) and immobilized dye molecules. All species show specific pH and ionic strength dependencies. A quantification of the individual species is difficult to realize. So, no clear statement regarding influence of the surface charge density σ can be given at the moment. Further systematic studies are necessary to quantify the effect.

In summary, both forms of the indicator are detected spectroscopically after immobilization of the styryl acridine derivative BS121 on CPG II, CPG III and CPG IV substrates. The response time is in the range of minutes and the CPG/indicator complexes show a pH-sensitivity over years. Furthermore, a relatively high ionic strength effect exists.

4. Summary

In this work, the use of porous glass membranes as matrix in optical chemical sensors was demonstrated. The membranes based on phase-separated alkali borosilicate glasses. Four different types of membranes with pore diameters of 12–112 nm were used. These possessed a thickness of 250 to 300 μm and dimensions of approximately $9 \times 13\ mm^2$. In a first step, the water permeability of selected membranes was determined gravimetrically. It appears that a Poiseuille flow occurs in the membranes if a pressure difference between 25 and 125 mbar was induced. The resultant flow through the membranes could be determined with reasonable accuracy if one assumes continuous pores and the law of Hagen–Poiseuille. Furthermore, the absorption spectra for water saturated membranes were recorded. In the case of wavelengths above 500 nm for membranes with pore diameter of more than 70 nm the self-absorption increased by 0.2 absorbance units.

The pH-sensitive CPG complexes were prepared on the basis of thymol blue and a styryl acridine derivative. The immobilization of thymol blue was performed according to [9]. The styryl acridine derivative was linked to the aminosilanized membranes using a NHS-ester. Due to the optical transparency of the membranes absorption spectra of the immobilized indicators were determined almost exactly. The formation of an isosbestic point was proven for both immobilized functional species. Furthermore, protonated and deprotonated forms of each indicator were recorded. The t_{90}-times of the thermodynamic equilibrium were determined in dependence on the pH value and ionic strength. The values varied between 4 and 23 min.

The influence of the ionic strength on the characteristic pH curve was discussed in detail. It was found that the ionic strength effects resulted from the combination of the styryl acridine derivative and the CPG membranes. The indicator was located within the charged interface inside the pores. Furthermore, the charge density of the pore surface showed a dependency on the pH value. In addition, it was found that the shape of the absorption spectrum depends on the CPG membranes' type. Variations in the immobilization procedure resulted in a change in the pH characteristic curve $E=f$ (pH), in a modified ionic strength effect and in different pK-values (between 4 and 5). An acceptable pH-sensitivity of the CPG/styryl acridine derivative complex was still detectable after about 900 days of storage.

In this work, the great potential of CPG membranes for applications in the field of optical chemo-sensors could be shown for the first time. Currently, the optimization of the membrane properties in terms of the response time: (i) membrane thickness, (ii) pore size, (iii) integration of a hierarchical pore structure and the immobilization of other functional species (enzymes, fluorescent dyes) are in the focus of several scientific studies.

References

[1] O.S. Wolfbeis, Fiber Optic Chemical Sensors and Biosensors, vol. 1, CRC-Press, Boca Raton, 1991.
[2] G. Boisde, A. Harmer, Chemical and Biochemical Sensing with Optical Fibers and Waveguides, Artech House Inc, Boston, 1996.
[3] G.J. Mohr, T. Nezel, U.E. Spichiger, Anal. Chim. Acta 414 (2000) 181–187.
[4] G.E. Baldini, K.T.V. Grattan, A.C.C. Tseung, Rev. Sci. Instrum. 66 (1995) 4034–4040.
[5] G. Schulz-Ekloff, D. Woehrle, B. Duffel, R.A. Schoonheydt, Microporous Mesoporous Mater. 51 (2002) 91–138.
[6] F. Janowski, D. Enke, in: F. Schueth, K.S.W. Sing, J. Weitkamp (Eds.), Handbook of Porous Solids, Wiley-VCH, Weinheim, 2002, p. 1431.
[7] F. Baldini, A. Falai, Optical Sensors and Microsystems: New Concepts, Materials, Technologies, in: S. Martellucci, A.N. Chester, A.G. Mignani (Eds.), Kluwer Academic Publishers, New York, 2000, pp. 53–60.
[8] M.P. Xavier, B. Vallejo, M.D. Marazuela, M.C. Moreno-Bondi, F. Baldini, A. Falai, Biosens. Bioelectron. 14 (2000) 895–905.
[9] R.T. Andres, R. Narayanaswamy, Talanta 44 (1997) 1335–1352.
[10] D. Enke, F. Friedel, F. Janowski, T. Hahn, W. Gille, R. Mueller, H. Kaden, in: F. Rodriguez-Reinoso, B. McEnaney, J. Rouquerol, K. Unger (Eds.), Characterization of Porous Solids VI. Studies in Surface Science and Catalysis, vol. 144, Elsevier, Amsterdam, 2002, p. 347.
[11] J.A. Coch Frugoni., Gazz. Chim. Ital. 87 (1957) 403–407.
[12] W. Fichtner, M. Berthold, R. Müller, H. Kaden, D. Enke, D. Jakob, T. Hahn, in: G. Gerlach, H. Kaden (Eds.), Dresdner Sensor-Symposium, 7, TUD press, Dresden, 2005, p. 279.
[13] Z. Foltynowicz, W. Urbaniak, B. Marciniec, F. Janowski, W. Heyer, Glass Technol. 34 (1993) 206–209.
[14] H. Chan, V. Aksyuk, R. Kleiman, D. Bishop, F. Capasso, Science 291 (2001) 1941–1944.
[15] J. Crank, The Mathematics of Diffusion, Oxford University Press, London, 1998.
[16] J.O.M. Bockris, A.K.N. Reddy, Modern Electrochemistry Ionics, vol. 1, Kluwer Academic Publishers, New York, 1998.
[17] J. Kärger, J. Lenzner, H. Pfeifer, H. Schwabe, W. Heyer, F. Janowski, F. Wolf, S.P. Zdanov, J. Am. Ceram. Soc. 66 (1982) 69.
[18] R.G. Bates, Determination of pH: Theory and Practice, John Wiley & Sons, New York, 1973.
[19] J. Janata, Anal. Chem. 59 (1987) 1351–1356.
[20] L. Ermakova, M. Sidorova, N. Jura, J. Membr. Sci. 115 (1996) 11–19.
[21] L. Ermakova, M. Sidorova, N. Jura, I. Savina, J. Membr. Sci. 131 (1997) 125–141.
[22] P.B. Wakeling, Appl. Opt. 18 (1979) 3208–3210.
[23] W. Janusz, A.L. Dawidowicz, J. Szczypa, J. Mater. Sci. 26 (1991) 4865–4868.